Workshop 2: Whirl Flutter Aeroservoelasticity

2024/2025 - Prof. Quaranta

Team members	Personal code
Matteo Baio	10667431
Gaia Lapucci	10710434
Lorenzo Lucatello	10735694

Introduction

The aim of this workshop is to visualize and analyze the aeroelastic behavior of the XV-15 prop-rotor. The behavior of the isolated rotor will first be investigated in terms of mode shapes and then the whole wing-rotor assembly will be analyzed in terms of both mode shapes and flutter characteristics. Finally, we studied the relevance of specific modes for the onset of whirl flutter.

Input Data

The airframe data and model were the same as the one used in the previous workshop. For the rotor instead, we were given a finite element model defined by 188 nodes and the respective connectivity elements. The modal mass matrix $\mathbf{M}_r$, the modal damping matrix $\mathbf{C}_r$, the modal stiffness matrix $\mathbf{K}_r$ and the eigenvectors were given as well. The model has 29 modes and for each mode the associated eigenvector is in the form of a 6×168 matrix, as we consider 6 degrees of freedom (3 translations and 3 rotations) for each node. The geometrical data of the prop-rotor is available in Table 1.

Radius	3.5 m
N. of blades	3
Solidity	0.10
NR	740 rpm

Table 1: Rotor data

Task 0: Load the airframe model

Task 0 was already provided to us and recalls what was carried out in the previous workshop. The only peculiarity was that the new system has an actuator stiffness of $K_{\text{act}} = 9800\,^{\text{Nm}}/_{\text{rad}}$ and an actuator damping of $C_{\text{act}} = 20\,^{\text{Nm}\cdot\text{s}}/_{\text{rad}}$.

Task 1: Load the rotor model

First we loaded the rotor data from the document `LabData_Session2_rotor.mat` and with the MATLAB® function `fullMeshVisualization.m` we created the visualization of the FEM model as shown in Figure 1. Then, by sorting the node displacements provided in the model data, and by using the function `fullAnimateModel.m` we were able to plot and animate the mode shapes.

Remark: The first two mode shapes are associated with the elastic deformation (translation) of the flexible support and the rigid deformation of the rotor. The third mode is instead associated with the elastic deformation of the flexible support in the thrust direction, which affects the pitch link mechanism and thus changes the pitch of the blades (collectively). There are also two modes, which represent the elastic deformation (rotation) of the flexible support which once again affects the pitch link mechanics but this time causes a cyclic change of the pitch angle.

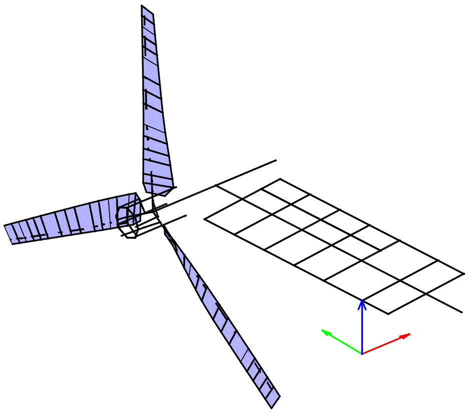

Figure 1: Finite element model

Remark: In order the describe the whirl flutter phenomenon, the bear minimum rotor modes that must be considered in the analysis are the first coning mode and the first lead-lag mode. Higher order modes are less relevant for the analysis.

Task 2: Compute the isolated rotor (grounded) modes

To compute the isolated rotor modes, we need to solve the eigenvalue problem associated to the generalized spring-mass-damper equation considering that the connection between the hub center and the swash plate center (respectively nodes 1 and 9500) are grounded and thus have no free degrees of freedom.

Considering the equation of the free dynamics of the rotor:

$$\mathbf{M}_{\mathrm{R}}\ddot{\mathbf{q}}_{\mathrm{r}} + \mathbf{C}_{\mathrm{R}}\dot{\mathbf{q}}_{\mathrm{r}} + \mathbf{K}_{\mathrm{R}}\mathbf{q}_{\mathrm{r}} = \mathbf{0}$$

The aim is to include in this equation that the nodes 1 and 9500 are grounded, thus imposing that $\mathbf{u}_1$ and $\mathbf{u}_{9500}$ are null and that is done with the elimination method. Recalling the definition of modal coordinates, we can write those displacements as:

$$\begin{bmatrix} \mathbf{u}_1 \\ \mathbf{u}_{9500} \end{bmatrix} = \mathbf{\Phi}_{\mathrm{R}}\mathbf{q}_{\mathrm{r}} = \mathbf{0}$$

We can partition the modal coordinates in two groups: $\mathbf{q}_{\mathrm{r}}^1$ and $\mathbf{q}_{\mathrm{r}}^2$ and accordingly also the eigenvectors will be separated into $\mathbf{\Phi}_{\mathrm{R}}^1$ and $\mathbf{\Phi}_{\mathrm{R}}^2$. In this way we are able to impose a compatibility condition between the two groups of modal coordinates:

$$\begin{bmatrix} \mathbf{\Phi}_{\mathrm{R}}^1 & \mathbf{\Phi}_{\mathrm{R}}^2 \end{bmatrix} \begin{bmatrix} \mathbf{q}_{\mathrm{r}}^1 \\ \mathbf{q}_{\mathrm{r}}^2 \end{bmatrix} = \mathbf{0} \quad \Longrightarrow \quad \mathbf{q}_{\mathrm{r}}^1 = -[\mathbf{\Phi}_{\mathrm{R}}^1]^{-1}\,\mathbf{\Phi}_{\mathrm{R}}^2\,\mathbf{q}_{\mathrm{r}}^2$$

Remark: The matrix $\mathbf{\Phi}_{\mathrm{R}}^1$ must be invertible.

Finally, to include this constraint in the free spring-mass-damper equation, we are first going to define the matrix $\mathbf{T}$ which integrates the constraint into the modal coordinates and therefore links the free modal coordinates $\mathbf{q}_{\mathrm{r}}$ into the constrained coordinates $\mathbf{q}_{\mathrm{r}}^1$ and $\mathbf{q}_{\mathrm{r}}^2$.

$$\begin{bmatrix} \mathbf{q}_{\mathrm{r}}^1 \\ \mathbf{q}_{\mathrm{r}}^2 \end{bmatrix} = \begin{bmatrix} -[\mathbf{\Phi}_{\mathrm{R}}^1]^{-1}\,\mathbf{\Phi}_{\mathrm{R}}^2 \\ \mathbb{I} \end{bmatrix} \mathbf{q}_{\mathrm{r}} = \mathbf{T}\,\mathbf{q}_{\mathrm{r}}$$

We recall then the spring-mass-damper equation decomposed based on the separation of the modal coordinates into $\mathbf{q}_{\mathrm{r}}^1$ and $\mathbf{q}_{\mathrm{r}}^2$:

$$\begin{bmatrix} \mathbf{M}_{11} & \mathbf{M}_{12} \\ \mathbf{M}_{21} & \mathbf{M}_{22} \end{bmatrix} \begin{bmatrix} \ddot{\mathbf{q}}_{\mathrm{r}}^1 \\ \ddot{\mathbf{q}}_{\mathrm{r}}^2 \end{bmatrix} + \begin{bmatrix} \mathbf{C}_{11} & \mathbf{C}_{12} \\ \mathbf{C}_{21} & \mathbf{C}_{22} \end{bmatrix} \begin{bmatrix} \dot{\mathbf{q}}_{\mathrm{r}}^1 \\ \dot{\mathbf{q}}_{\mathrm{r}}^2 \end{bmatrix} + \begin{bmatrix} \mathbf{K}_{11} & \mathbf{K}_{12} \\ \mathbf{K}_{21} & \mathbf{K}_{22} \end{bmatrix} \begin{bmatrix} \mathbf{q}_{\mathrm{r}}^1 \\ \mathbf{q}_{\mathrm{r}}^2 \end{bmatrix}$$

We then substitute the constraining equation and obtain:

$$\mathbf{T}^T \begin{bmatrix} \mathbf{M}_{11} & \mathbf{M}_{12} \\ \mathbf{M}_{21} & \mathbf{M}_{22} \end{bmatrix} \mathbf{T}\ddot{\mathbf{q}}_\mathrm{r} + \mathbf{T}^T \begin{bmatrix} \mathbf{C}_{11} & \mathbf{C}_{12} \\ \mathbf{C}_{21} & \mathbf{C}_{22} \end{bmatrix} \mathbf{T}\dot{\mathbf{q}}_\mathrm{r} + \mathbf{T}^T \begin{bmatrix} \mathbf{K}_{11} & \mathbf{K}_{12} \\ \mathbf{K}_{21} & \mathbf{K}_{22} \end{bmatrix} \mathbf{T}\mathbf{q}_\mathrm{r} = \mathbf{0}$$

In this way we are able to define the constrained mass, damping and stiffness matrices.

$$\mathbf{M}_\mathrm{restr}\ddot{\mathbf{q}}_\mathrm{r} + \mathbf{C}_\mathrm{restr}\dot{\mathbf{q}}_\mathrm{r} + \mathbf{K}_\mathrm{restr}\mathbf{q}_\mathrm{r} = \mathbf{0}$$

To then compute the new modal frequencies and modal shapes, we build the associated state space system and then find the eigenvalues and eigenvectors of matrix $\mathbf{A}$ using the MATLAB® function `eig( )`.

$$\begin{bmatrix} \dot{\mathbf{q}}_\mathrm{r} \\ \ddot{\mathbf{q}}_\mathrm{r} \end{bmatrix} = \begin{bmatrix} \mathbf{0} & \mathbb{I} \\ -\mathbf{M}_\mathrm{restr}^{-1}\mathbf{K}_\mathrm{restr} & -\mathbf{M}_\mathrm{restr}^{-1}\mathbf{C}_\mathrm{restr} \end{bmatrix} \begin{bmatrix} \mathbf{q}_\mathrm{r} \\ \dot{\mathbf{q}}_\mathrm{r} \end{bmatrix}$$

Here follows, in Figure 2 the polar plot of the most significant eigenvalues.

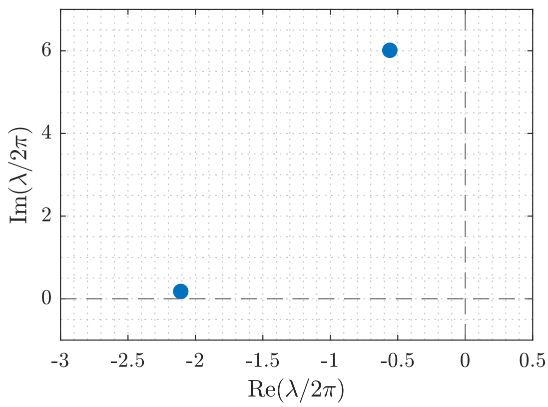

Figure 2: Polar plot of the isolated rotor eigenvalues

In order to plot the modal shapes, we need to take into account that the eigenvectors are complex. This add complexity in the evaluation of the displacements of the nodes. Indeed, considering that the eigenvector components are complex conjugate pairs, the displacement is given by the sum of two eigenvector complex conjugate pairs scaled by the respective eigenvalue:

$$(v_{ij} + \bar{v}_{ij})\lambda_i = \mathrm{real}\left((A + iB)e^{(s+i\omega)t} + (A - iB)e^{(s+i\omega)t}\right) = \ \dots\ = 2\left(A\cos(\omega t) - B\sin(\omega t)\right)e^{st}$$

Because we want to plot the modes not considering scaling terms, and because the term e^{st} is just a time varying scaling constant, we can omit this term when plotting the modes.

Here follows, in Figure 3, 4, 5 and 6 the isolated rotor modal shapes:

Remark: The matrix $-[\mathbf{\Phi}_\mathrm{R}^1]^{-1}\,\mathbf{\Phi}_\mathrm{R}^2$ is a 12×17 null matrix. The explanation is that the displacements of the different nodes are independent and perpendicular to each other. Considering the 12 modes affected by the above matrix, each of them influences a single degree of freedom of the two connection nodes (12 degrees of freedom overall).

Task 3: Connect the rotor to the wing

To connect the rotor to the wing we have to add a constraint equation for which the displacements of the swashplate and hub nodes of the rotor are equal to the swashplate and hub nodes of the airframe which are respectively node number 100000 and 1000007. Therefore the constraint equation is:

$$\begin{bmatrix} \mathbf{u}_1 \\ \mathbf{u}_{9500} \end{bmatrix} = \begin{bmatrix} \mathbf{u}_{100000} \\ \mathbf{u}_{1000007} \end{bmatrix}$$

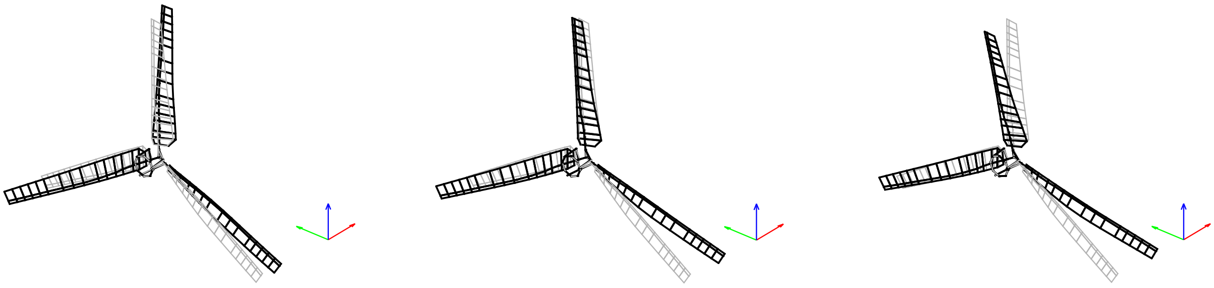

Figure 3: 1st modal shapes of the isolated rotor

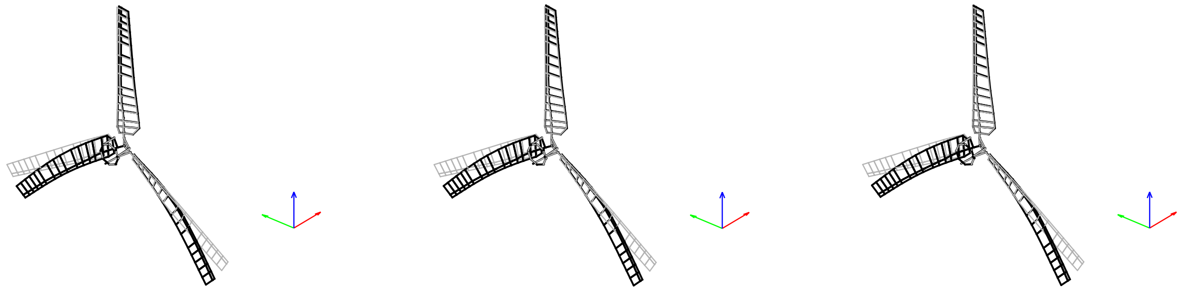

Figure 4: 2nd modal shapes of the isolated rotor

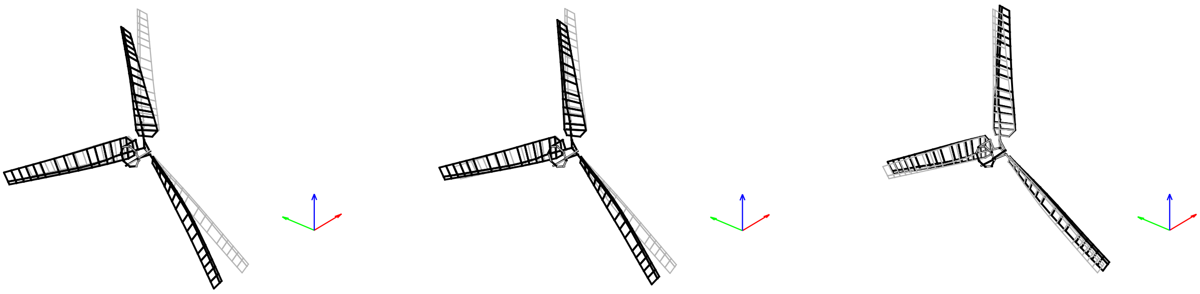

Figure 5: 3rd modal shapes of the isolated rotor

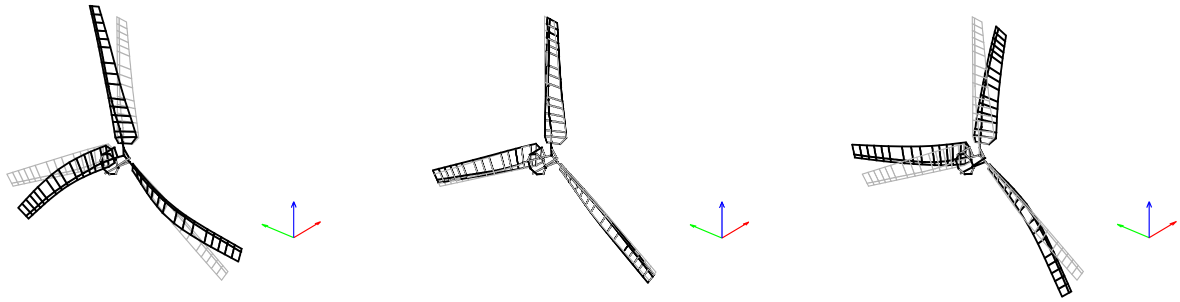

Figure 6: 4th modal shapes of the isolated rotor

By using once again the modal coordinates to define the displacements of the airframe nodes and by recalling the previous definition of the rotor displacements with partitioned modal coordinates we developed the following constraint equation:

$$[\mathbf{\Phi}_\mathrm{R}^1 \quad \mathbf{\Phi}_\mathrm{R}^2]\begin{bmatrix}\mathbf{q}_\mathrm{r}^1\\ \mathbf{q}_\mathrm{r}^2\end{bmatrix} = \mathbf{\Phi}_\mathrm{A}\mathbf{q}_\mathrm{a} \quad \Longrightarrow \quad \mathbf{q}_\mathrm{r}^1 = [\mathbf{\Phi}_\mathrm{R}^1]^{-1}[\mathbf{\Phi}_\mathrm{A}\mathbf{q}_\mathrm{a} - \mathbf{\Phi}_\mathrm{R}^2\ \mathbf{q}_\mathrm{r}^2]$$

This constraint was then added inside the uncoupled partitioned spring-mass-damper equation to recover the constrained mass, damping and stiffness matrices. The procedure was the same as for the previous task.

$$\begin{bmatrix}\mathbf{q}_\mathrm{a}\\ \mathbf{q}_\mathrm{r}^1\\ \mathbf{q}_\mathrm{r}^2\end{bmatrix} = \begin{bmatrix}\mathbb{I} & \mathbf{0}\\ [\mathbf{\Phi}_\mathrm{R}^1]^{-1}\mathbf{\Phi}_\mathrm{A} & -[\mathbf{\Phi}_\mathrm{R}^1]^{-1}\mathbf{\Phi}_\mathrm{R}^2\\ \mathbf{0} & \mathbb{I}\end{bmatrix}\begin{bmatrix}\mathbf{q}_\mathrm{a}\\ \mathbf{q}_\mathrm{r}\end{bmatrix} = \mathbf{T}\begin{bmatrix}\mathbf{q}_\mathrm{a}\\ \mathbf{q}_\mathrm{r}\end{bmatrix}$$

Recalling the uncoupled partitioned spring-mass-damper equation:

$$\begin{bmatrix}\mathbf{M}_{hh} & \mathbf{0} & \mathbf{0}\\ \mathbf{0} & \mathbf{M}_{11} & \mathbf{M}_{12}\\ \mathbf{0} & \mathbf{M}_{21} & \mathbf{M}_{22}\end{bmatrix}\begin{bmatrix}\ddot{\mathbf{q}}_\mathrm{a}\\ \ddot{\mathbf{q}}_\mathrm{r}^1\\ \ddot{\mathbf{q}}_\mathrm{r}^2\end{bmatrix} + \begin{bmatrix}\mathbf{C}_{hh} & \mathbf{0} & \mathbf{0}\\ \mathbf{0} & \mathbf{C}_{11} & \mathbf{C}_{12}\\ \mathbf{0} & \mathbf{C}_{21} & \mathbf{C}_{22}\end{bmatrix}\begin{bmatrix}\dot{\mathbf{q}}_\mathrm{a}\\ \dot{\mathbf{q}}_\mathrm{r}^1\\ \dot{\mathbf{q}}_\mathrm{r}^2\end{bmatrix} + \begin{bmatrix}\mathbf{K}_{hh} & \mathbf{0} & \mathbf{0}\\ \mathbf{0} & \mathbf{K}_{11} & \mathbf{K}_{12}\\ \mathbf{0} & \mathbf{K}_{21} & \mathbf{K}_{22}\end{bmatrix}\begin{bmatrix}\mathbf{q}_\mathrm{a}\\ \mathbf{q}_\mathrm{r}^1\\ \mathbf{q}_\mathrm{r}^2\end{bmatrix} = \mathbf{0}$$

And substituting the constraint equation:

$$\mathbf{T}^T\begin{bmatrix}\mathbf{M}_{hh} & \mathbf{0} & \mathbf{0}\\ \mathbf{0} & \mathbf{M}_{11} & \mathbf{M}_{12}\\ \mathbf{0} & \mathbf{M}_{21} & \mathbf{M}_{22}\end{bmatrix}\mathbf{T}\begin{bmatrix}\ddot{\mathbf{q}}_\mathrm{a}\\ \ddot{\mathbf{q}}_\mathrm{r}\end{bmatrix} + \mathbf{T}^T\begin{bmatrix}\mathbf{C}_{hh} & \mathbf{0} & \mathbf{0}\\ \mathbf{0} & \mathbf{C}_{11} & \mathbf{C}_{12}\\ \mathbf{0} & \mathbf{C}_{21} & \mathbf{C}_{22}\end{bmatrix}\mathbf{T}\begin{bmatrix}\dot{\mathbf{q}}_\mathrm{a}\\ \dot{\mathbf{q}}_\mathrm{r}\end{bmatrix} + \mathbf{T}^T\begin{bmatrix}\mathbf{K}_{hh} & \mathbf{0} & \mathbf{0}\\ \mathbf{0} & \mathbf{K}_{11} & \mathbf{K}_{12}\\ \mathbf{0} & \mathbf{K}_{21} & \mathbf{K}_{22}\end{bmatrix}\mathbf{T}\begin{bmatrix}\mathbf{q}_\mathrm{a}\\ \mathbf{q}_\mathrm{r}\end{bmatrix} = \mathbf{0}$$

$$\Longrightarrow \mathbf{M}_\mathrm{restr}\begin{bmatrix}\ddot{\mathbf{q}}_\mathrm{a}\\ \ddot{\mathbf{q}}_\mathrm{r}\end{bmatrix} + \mathbf{C}_\mathrm{restr}\begin{bmatrix}\dot{\mathbf{q}}_\mathrm{a}\\ \dot{\mathbf{q}}_\mathrm{r}\end{bmatrix} + \mathbf{K}_\mathrm{restr}\begin{bmatrix}\mathbf{q}_\mathrm{a}\\ \mathbf{q}_\mathrm{r}\end{bmatrix} = \mathbf{0}$$

To then compute the new modal frequencies and modal shapes, we proceeded as mentioned in the previous task: we built the state space formulation of the system and then computed the eigenvalues and eigenvectors of the $\mathbf{A}$ matrix.

$$\mathbf{q}_\mathrm{t} = \begin{bmatrix}\mathbf{q}_\mathrm{a}\\ \mathbf{q}_\mathrm{r}\end{bmatrix} \quad \Longrightarrow \quad \begin{bmatrix}\dot{\mathbf{q}}_\mathrm{t}\\ \ddot{\mathbf{q}}_\mathrm{t}\end{bmatrix} = \begin{bmatrix}\mathbf{0} & \mathbb{I}\\ -\mathbf{M}_\mathrm{restr}^{-1}\mathbf{K}_\mathrm{restr} & -\mathbf{M}_\mathrm{restr}^{-1}\mathbf{C}_\mathrm{restr}\end{bmatrix}\begin{bmatrix}\mathbf{q}_\mathrm{t}\\ \dot{\mathbf{q}}_\mathrm{t}\end{bmatrix}$$

Here follows, in Figure 7 the polar plot of the most significant eigenvalues.

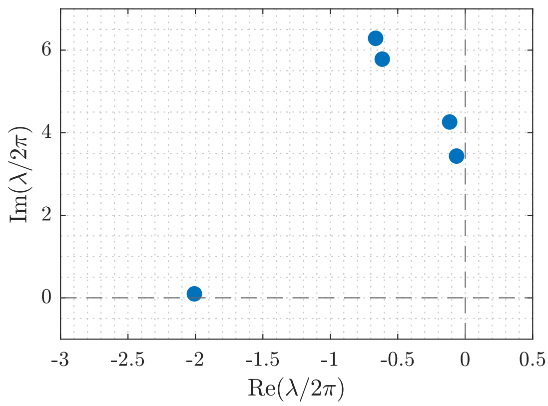

Figure 7: Polar plot of the rotor-airframe eigenvalues

As in the previous task, we have to take into account that the eigenvectors are complex. Here follows, in Figure 8,9,10 and 11 the combined rotor-airframe modal shapes.

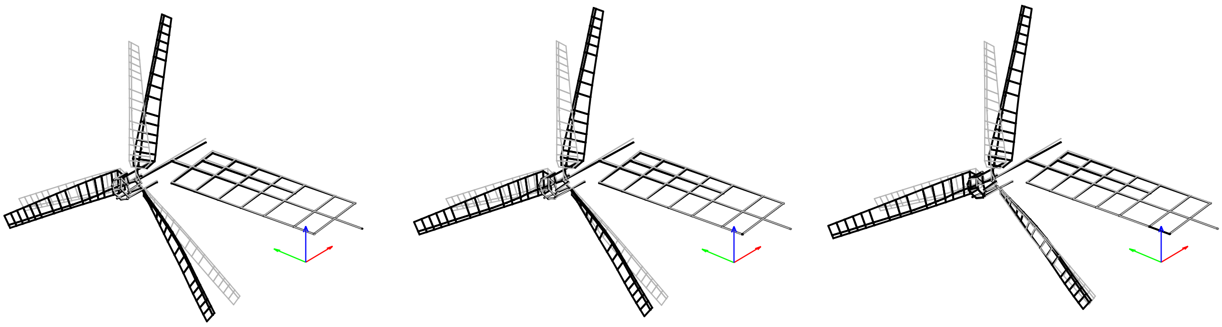

Figure 8: Combined rotor-airframe 1st mode shapes

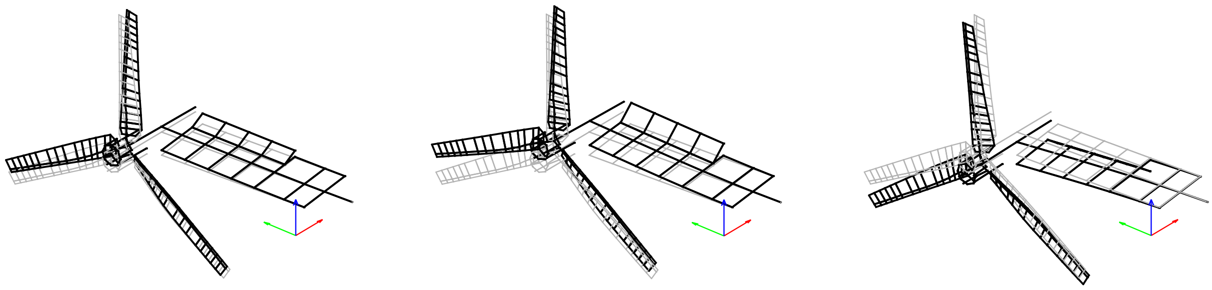

Figure 9: Combined rotor-airframe 2nd mode shapes

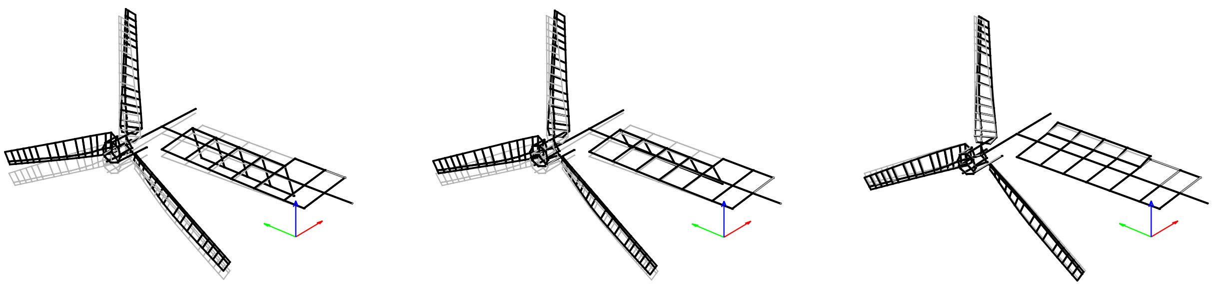

Figure 10: Combined rotor-airframe 3rd mode shapes

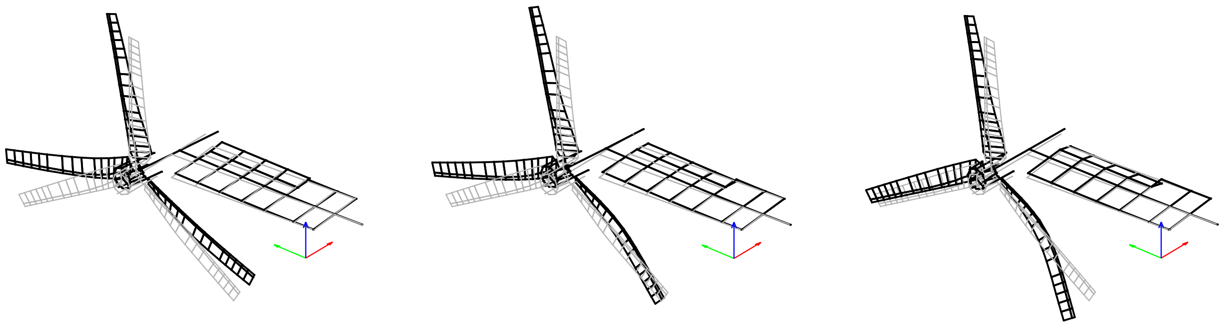

Figure 11: Combined rotor-airframe 4th mode shapes

Task 4: Whirl flutter

Function `load` was used to import the matrices in MATLAB®. The various matrices parametrized with airspeed were grouped within a single structure. Then we implemented what was already done in task 3, but just iterated inside a `for` loop for the various flight speeds. The eigenvalues were then plotted in Figure 12.

The following step was to remove the gimbal modes. Such modes refer to the ones associated with the rotor

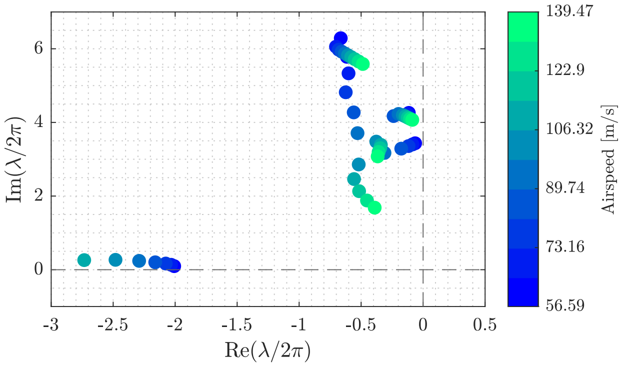

Figure 12: Rotor-airframe eigenvalues polar plot

movement allowed by the constant-velocity-joint (gimbal). Such mechanical component allows the rotor to have extra degrees of freedom, allowing it to rotate with respect to the wing. To remove these modes we took the matrix T and eliminated the columns associated to first two rotor modes. Repeating the previous analysis we then plotted the new eigenvalues in Figure 13.

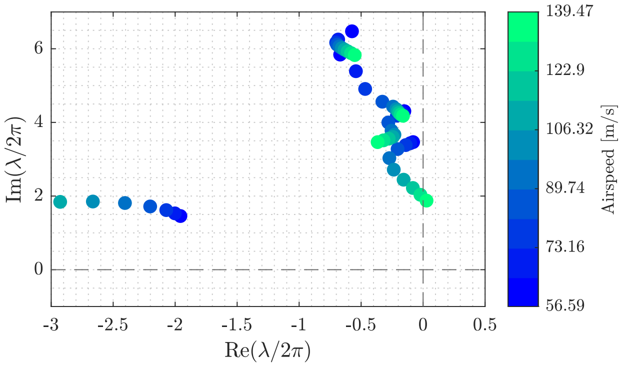

Figure 13: Rotor-airframe eigenvalues polar plot (no gimbal)

Remark: As we can see one of the eigenvalues has a positive real part suggesting the onset of whirl flutter. This phenomenon is expected because the gimbal modes have generally (but not always) a stabilizing effect. By removing such modes, the stability derivatives generally degrade resulting in a dynamic instability. It is particularly important to mention that is not always granted that the gimbal modes have a stabilizing effect. This property is case-dependent.

We identified that the mode that was going into flutter was the the second one. As follows, in Figure **??**, we have plotted the mode shape of the unstable mode.

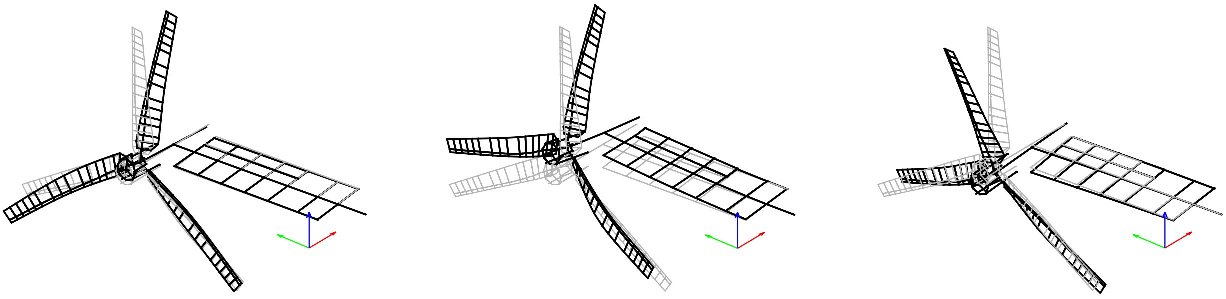

Figure 14: Whirl flutter 1st mode shape

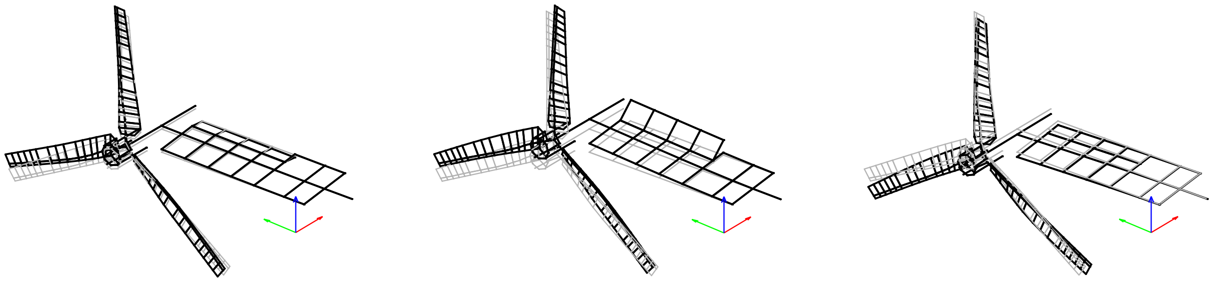

Figure 15: Whirl flutter 2nd mode shape

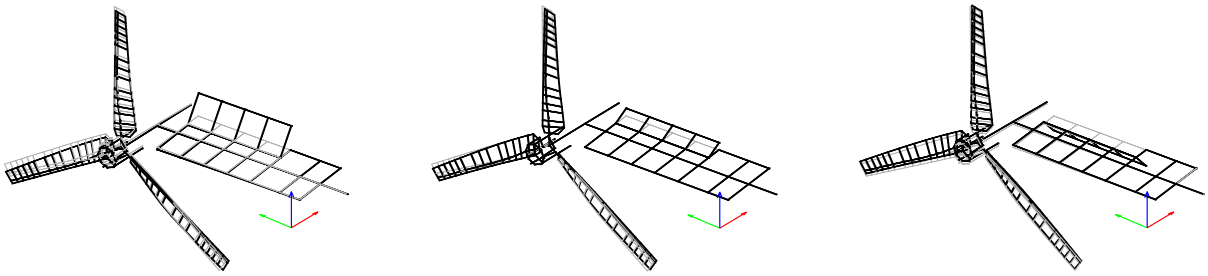

Figure 16: Whirl flutter 3rd mode shape

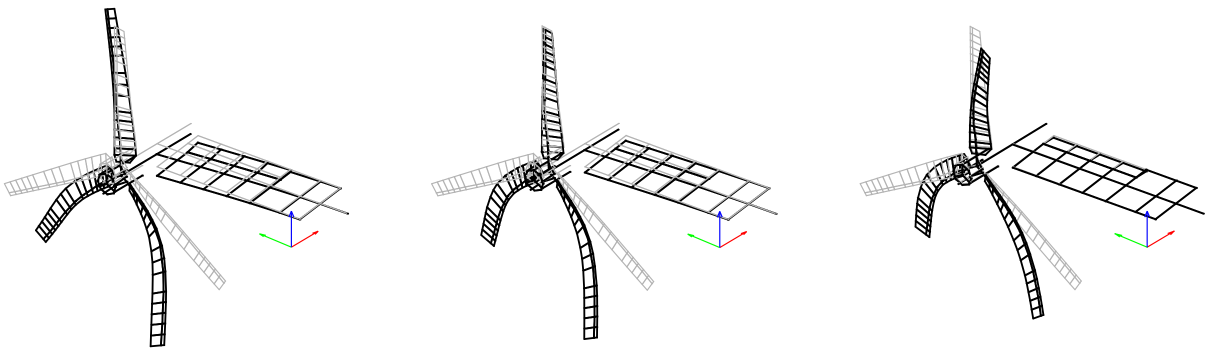

Figure 17: Whirl flutter 4th mode shape

We then removed the three largest high frequency modes of the airframe and, as expected, the system was still unstable (whirl flutter). This is important because it tells us that the relevant modes are just the gimbal ones. This procedure is typically applied in aeroelastic analysis to reduce the order of the model to a minimum allowing to better understand the key degrees of freedom that influence the aircraft's response. Usually the most influent are the ones whose removal completely changes the phenomenon; in our case those dofs are the gimbal ones.

Remark: Due to the central role of the gimbal modes in the stability of the aircraft, it's important to underline the relevance of the reliability of the constant-velocity-joint. Such component indeed represents a single point of failure that could lead to catastrophic consequences.

Work partition

The workshop was carried out in full cooperation between the team members. The codes of all tasks were developed and cross-checked together as well as the drafting of the report. For this reason it is not possible to allocate the single contributions of each team member.